Journal of Pharmacy and Pharmacology 3 (2015) 489-501
doi: 10.17265/2328-2150/2015.10.006

MTDLs Design on AChE (Acetylcholinesterase) and β-Secretase (BACE-1): 3D-QSAR and Molecular Docking Studies

Jiancheng Shi, Wentong Tu, Jiarong Sheng and Chusheng Huang

College of Chemistry and Material Sciences, Guangxi Teachers Education University, Nanning 530001, China

Abstract: To find promising new multitargeted AD (Alzheimer's disease) inhibitors, the 3D-QSAR (three-dimensional quantitative structure-activity relationship) model for 32 AD inhibitors was established by using the CoMFA (comparative molecular field analysis) and CoMSIA (comparative molecular similarity index analysis) methods. Results showed that the CoMFA and CoMSIA models were constructed successfully with a good cross-validated coefficient (q^2) and a non-cross-validated coefficient (R^2), and the binding modes obtained by molecular docking were in agreement with the 3D-QSAR results, which suggests that the present 3D-QSAR model has good predictive capability to guide the design and structural modification of novel multitargeted AD inhibitors. Meanwhile, we found that one side of inhibitory molecule should be small group so that it would be conductive to enter the gorge to interact with the catalytic active sites of AChE (acetylcholinesterase), and the other side of inhibitory molecule should be large group so that it would be favorable for interaction with the peripheral anionic site of AChE. Furthermore, based on the 3D-QSAR model and the binding modes of AChE and β-secretase (BACE-1), the designed molecules could both act on dual binding sites of AChE (catalytic and peripheral sites) and dual targets (AChE and BACE-1). We hope that our results could provide hints for the design of new multitargeted AD derivatives with more potency and selective activity.

Key words: 3D-QSAR, molecular docking, AChE, BACE-1, MTDLs.

1. Introduction

In the fight against AD (Alzheimer's disease), the etiology of AD has yet to be fully elucidated, and there is compelling evidence that this neurodegenerative disease is a multifactorial syndrome [1, 2]. Therefore, pharmaceutical researchers have proposed a move from the "one protein, one target, one drug" strategy to the "one drug, multiple targets" paradigm, which suggests the use of compounds with multiple activities at different target sites. Accordingly, the MTDLs (multitarget-directed ligands) design strategy has been the subject of increasing attention by many research groups [3-8]. An *in vitro* and *in vivo* characterization revealed its multifunctional mechanism of action and its interaction with three molecular targets involved in AD pathology, namely, AChE (acetylcholinesterase), Aβ (β-amyloid), and β-secretase (BACE-1) [8, 9].

Up to now, the MTDLs design strategy has proven particularly fruitful, some of which have emerged as interesting pharmacological tools for the investigation of neurodegenerative disorders, or as innovative drug candidates for combating AD [3-7]. For example, Hui et al. [4] reported that design and synthesis of tacrine-phenothiazine hybrids as multitarget drugs for Alzheimer's disease. Rosini et al. [5] studied that multi-target design strategies in the context of Alzheimer's disease: acetylcholinesterase inhibition and NMDA receptor antagonism as the driving forces. Bolea et al. [6] stated propargylamine-derived multitarget-directed ligands: fighting Alzheimer's disease with monoamine oxidase inhibitors.

In order to further elucidate the binding mechanism

Corresponding author: Chusheng Huang, Ph.D, professor, research fields: organic synthesis and natural products. E-mail: wyc666999@sina.cn.

of multitargeted AD inhibitors, molecular docking and 3D-QSAR (three-dimensional quantitative structure-activity relationship) studies should be carried out [10]. Molecular docking is an efficient tool for investigating receptor-ligand interactions, which plays a key role in clarifying the mechanism of molecular recognition in order to improve some biological function for the design of new compounds, especially when the crystal structure of a receptor or enzyme is available [11, 12]. The aim of 3D-QSAR modeling is that the developed model should be strong enough to be capable of making accurate and reliable predictions of biological activities of new compounds [13].

In this context, we focused on finding new MTDLs with high potency and selective activity on AChE (anticholinesterase) and *β*-secretase (BACE-1). Based on the docked conformations within the active sites of AChE and BACE-1, the 3D-QSAR analyses were performed directly using both the CoMFA (comparative molecular field analysis) and CoMSIA (comparative molecular similarity index analysis) models. Through a detailed understanding of their biological characteristics and their mechanism of action, we expect to provide more information for the structural modification of new multitargeted AD (Alzheimer's disease) inhibitors and theoretical guidance for carrying out rational clinical drug treatment for AD [14-16].

2. Materials and Methods

In the present work, the 32 compounds in *in vitro* reported by Bolognesi et al. [1, 2, 8, 17] were taken for the study, and their structures and bioactivities were listed in Table 1 (A1-A6 [17], B1-B8 [2], C1-C3 [8], D1-D7 [1], E1-E8 [8]). Four compounds in Table 1 were randomly selected as an external test set for further model validation, and the rest of the 28 compounds served as a training set to build the 3D-QSAR model.

The 3D structures of these compounds were sketched with molecular modeling software package SYBYL-X2.0 [18] and energetically minimized using the Tripos force field with Gasteiger-Hückel charges [10]. The 3D-QSAR model and molecular docking were carried out with the software package SYBYL-X2.0 [18]. The crystal structures of human AChE complexed with donepezil (E20) and human BACE-1 complexed with AZD3835 (32D) were retrieved from PDB with corresponding entry code 4EY7 [19] and 4B05 [20], respectively (http://www.pdb.org/). In order to compare the results from docking protocols and obtain good docking score, the donepezil and AZD3835 ligands were removed from donepezil-AChE complex and AZD3835-BACE-1 complex, respectively, and then the hydrogen atoms were added on the AChE and BACE-1 enzymes, respectively. Other parameters were established by default in software.

3. Results and Discussion

3.1 3D-QSAR Study

3.1.1 CoMFA and CoMSIA Model

For CoMFA model, steric and electrostatic fields were probed using a sp^3 carbon atom with a +1.0 net charge atom and a distance-dependent dielectric at each lattice point. The steric and electrostatic contributions were truncated at a default value of 30.0 kcal/mol and the latter were ignored at the lattice intersections with the maximal steric interactions [21, 22].

For CoMSIA model, it was derived with the same lattice box as used for the CoMFA calculations. Five physicochemical properties (steric (S), electrostatic (E), hydrophobic (H), hydrogen bond donor (D), and hydrogen bond acceptor (A)) were evaluated using the probe atom. A probe atom sp3 carbon with a charge of +1, hydrophobicity of +1, and H-bond donor and acceptor property of +1 was placed at every grid point to measure the S, E, H, D and A fields [21]. In this paper, the statistical results showed that the CoMSIA model by SEHD combination gave the highest

Table 1 Structures and predicted activities of 32 inhibitors.

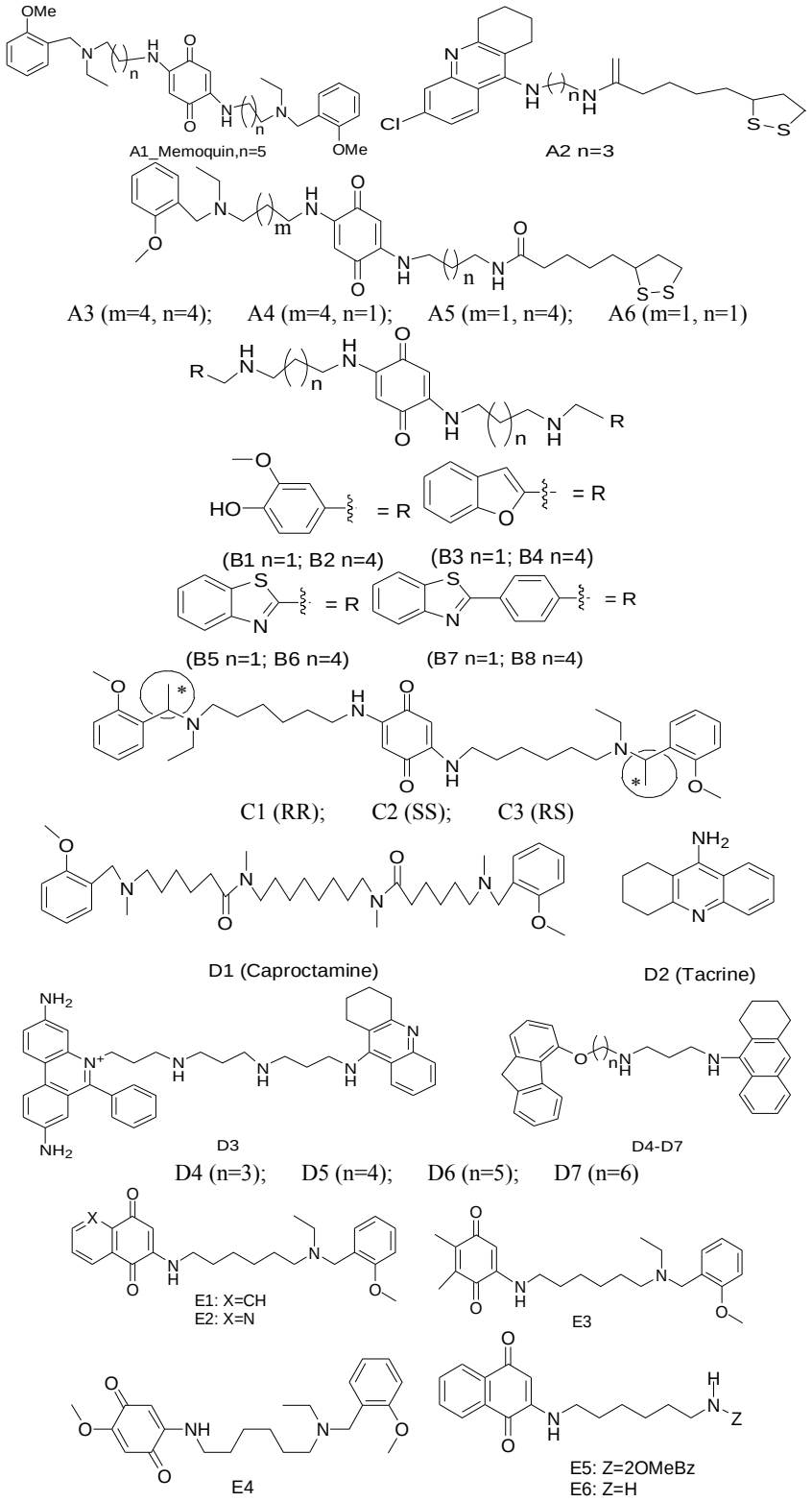

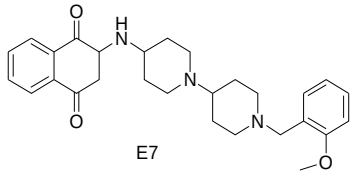

E7

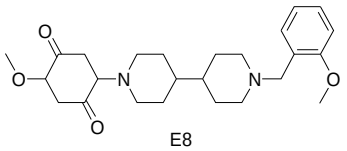

E8

Compound	IC_{50}(nM)	PIC_{50}(EA)[a]	PIC_{50}(PA)[b]	Residual[c]	T_S[d]	T_S[e]
A1(Memoquin)	1.55	8.8097	8.859	-0.05	8.06	9.16
A2	0.253	9.5969	9.58	0.017	5.25	6.55
A3	100	7.0000	7.003	-0.003	6.99	8.73
A4	150	6.8239	6.802	0.022	6.93	8.62
A5	160	6.7959	6.793	0.003	7.92	8.86
A6	190	6.7212	6.746	-0.025	7.36	9.51
B1	198	6.7033	6.691	0.012	9.16	5.92
B2	102	6.9914	6.979	0.012	4.53	6.76
B3	21800	4.6615	4.667	-0.006	5.09	7.69
*B4	>>10		6.283		3.12	7.02
*B5	>>10		6.435		3.07	4.56
B6	22000	4.6576	4.636	0.021	5.15	6.82
B7	31400	4.5031	4.505	-0.002	6	4.61
B8	305	6.5157	6.524	-0.008	9.07	8.9
C1(RR)	0.5	9.3010	9.252	0.049	8.14	11.42
C2(SS)	4.03	8.3947	8.365	0.0291	7.95	10.86
C3(RS)	0.36	9.4437	9.491	-0.047	10.42	10.6
*D1(Caproctamine)	170	6.7696	7.127	-0.357	6.65	10.46
*D2(Tacrine)	424	6.3726	6.662	-0.289	5.42	3.58
D3	1.55	8.8097	8.817	-0.007	6.48	8.19
D4	2.15	8.6676	8.647	0.02	8.08	6.05
D5	1.65	8.7825	8.794	-0.011	4.73	7.61
D6	1.54	8.8125	8.845	-0.032	5.76	8.41
D7	2.57	8.5901	8.575	0.015	6.08	7.82
E1	9.73	8.0119	7.919	0.093	6.11	6.47
E2	27.9	7.5544	7.601	-0.047	6.19	7.83
E3	29	7.5376	7.597	-0.059	3.83	5.77
E4	65.3	7.1851	7.165	0.02	4.8	6.24
E5	1850	5.7328	5.716	0.017	5.73	5.85
E6	64500	4.1904	4.193	-0.003	5.78	5.44
E7	17200	4.7645	4.764	0.0005	7.27	8.47
E8	24400	4.6126	4.643	-0.031	6.51	8.35

*Samples in the test set; a: Experimental activity (PIC50); b: Predicted activity (PIC50); c: The residual difference between experimental and predicted activities; d: Docking total_score on AChE; e: Docking total_score on BACE-1.

cross-validated value (q2), correlation coefficient (R2) and fischer test value (F), which means that the SEHD combination has the best prediction ability and stability. Therefore, we chose SEHD combination to establish the best CoMSIA model. Meanwhile, the statistical evaluation for the CoMSIA analyses was executed in the same way as described for CoMFA [10].

3.1.2 PLS (Partial Least-Square) Calculations and Validations

The relationship between the CoMFA and CoMSIA interaction energies and the AChE inhibitory activity (pIC50) has been quantified by the PLS (partial least-square) method (leave-one-out) [21, 23]. The cross-validated q^2 that resulted in the NOC (optimum number of components) and lowest standard error of

prediction was selected. The minimum column filtering value was set to 2.0 kcal/mol to speed up the analysis with improvement signal-to-noise ratio. Final analysis was performed to calculate non-cross-validated (R^2) using the optimum NOC obtained from the leave-one-out cross-validation analysis [10, 21, 23].

3.1.3 CoMFA and CoMSIA Model Analysis

The results of PLS analysis were summarized in Table 2. Often, a high q^2 value ($q^2 > 0.5$) is considered as a proof of the high predictive ability of the model [24, 25]. As shown in Table 2, the q^2 values of CoMFA and CoMSIA models are 0.535 and 0.537, respectively, which suggests that the CoMFA and CoMSIA models have strong predictive ability [26]. Meanwhile, we could observe from Fig. 1 that the predicted values using the newly constructed CoMFA and CoMSIA models were in well agreement with experimental data, which reveals that the CoMFA and CoMSIA models are reliable [26]. Furthermore, it could be obtained from Fig. 1 that the correlation coefficient (R^2) is 0.999 for CoMFA model (Fig. 1a), while 0.992 for CoMSIA model (Fig. 1b). The result means that the CoMFA model is more reliable than CoMSIA model. Therefore, the CoMFA model was employed to design new inhibitors in the present work.

Based on above 3D-QSAR model, the CoMFA and CoMSIA coefficient isocontour maps were made onto the active sites of enzyme (AChE) in Figs. 2 and 3, respectively [10]. One notes that the B series inhibitors in Table 1 were chosen as examples to validate the predictive capability of 3D-QSAR model, and the compound B2 (the most potent inhibitor of B series) was used as a reference molecule in Figs. 2 and 3 [10]. Table 2 shows that the CoMFA steric field descriptor explains 51.9% of the variance, while the electrostatic descriptor explains the rest 48.1%. These steric and electrostatic fields were presented as contour plots in Figs. 2a and 2b, respectively [26].

As seen from the contour plot of CoMFA steric field in Fig. 2a, the bulky substituent in green regions (favor steric) would be favorable for inhibitory potency, while bulky substituent in yellow regions (disfavor steric) would not be beneficial to inhibitory activity. In particular, there are two interesting features

Table 2 Statistical indexes of CoMFA (comparative molecular field analysis) and CoMSIA (comparative molecular similarity index analysis) models based on 32 compounds.

Model	q^2	Optimal number of components	R^2	F	QSAR field distribution (%)
CoMFA	0.535	13	0.999	2963.199	S:0.519; E:0.481
CoMSIA	0.537	7	0.992	383.709	S:0.193; E:0.295; H:0.296; D:0.217

q^2: the cross-validated value; R^2: correlation coefficient; F: Fischer test value.

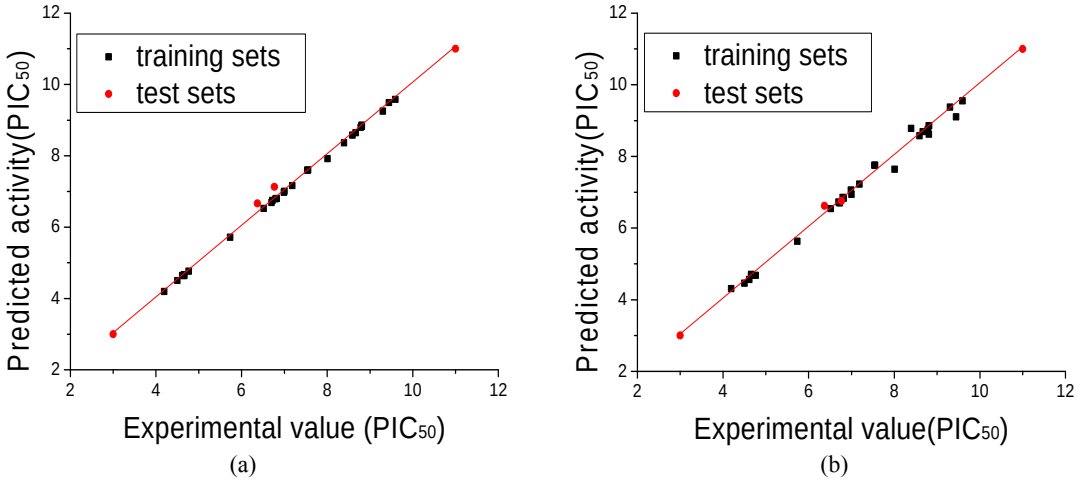

Fig. 1 The experimental PIC_{50} versus the predicted PIC_{50} by CoMFA (a) and CoMSIA (b) models.

exhibited in Fig. 2a: (i) The right vanillic group located in large green region, while the left one located in small green region; (ii) The right carbon chain located in large yellow region, while the left one does not. The result suggests that one side of inhibitor should be small group so that it would be conductive to enter the gorge to interact with the catalytic active sites, and the other side of inhibitor should be large group so that it would be favorable for interaction with the peripheral anionic site.

From the contour plot of CoMFA electrostatic field in Fig. 2b, the blue is the electropositive favored color, and the red is the electronegative favored color. Fig. 2b reveals that the electronegative substituents should be distributed around the right and left imino-groups near the vanillic group, while the electropositive substituents should be distributed around two carbonyl of benzoquinone [24, 27].

As shown in Table 2, the steric field descriptor explains 19.3% of the variance, while the proportion of electrostatic field, hydrophobic field and hydrogen bond donor field descriptors account for 29.5%, 29.6% and 21.6%, respectively [26]. It could be seen from the CoMSIA contour map in Fig. 3 that, the CoMSIA steric (Fig. 3a) and electrostatic (Fig. 3b) fields were in accordance with the distribution of the CoMFA steric (Fig. 2a) and electrostatic (Fig. 2b) fields, respectively. However, as comparative with Fig. 2b, the area of red (favor electronegative) was small in Fig. 3b. As for the difference, it might be highly probable the reason that the hydrophobic and other factors would affect the inhibitory activity [26].

The contour plot of CoMSIA hydrophobic field in Fig. 3c displays that the methoxyls and hydroxyls of two vanillic groups all located in white regions (favor hydrophilic), which means that inhibitory potency would be enhanced when the substituent groups were more hydrophilic. The right carbon chain of benzoquinone located in yellow regions, suggesting that the hydrophobic groups in this region might improve inhibitory potency.

According to the contour plot of CoMSIA bond donor field in Fig. 3d, left imino-group near the benzoquinone and carbonyl on benzoquinone both located in cyan regions, which reveals that hydrogen bond donor groups around there could improve inhibitory activity. The right imino-group near the vanillic group located in purple region. The result demonstrates that the hydrogen bond donor groups around there would not be conducive to inhibitory activity.

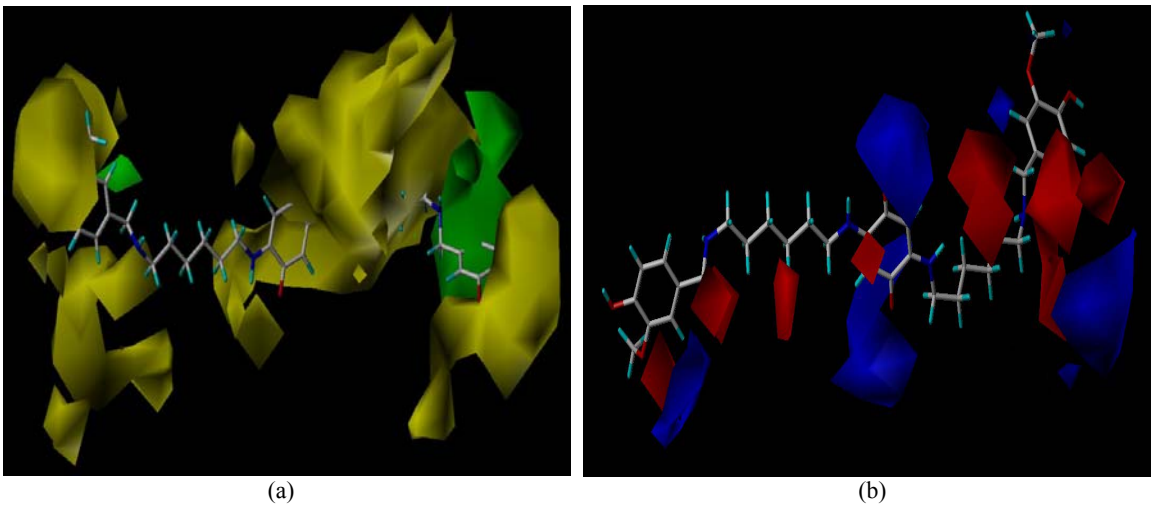

(a) (b)

Fig. 2 CoMFA contour maps around compound B2. (a) Steric field (green: steric favored; yellow: steric disfavored); (b) Electrostatic field (blue: electropositive favored; red: electronegative favored).

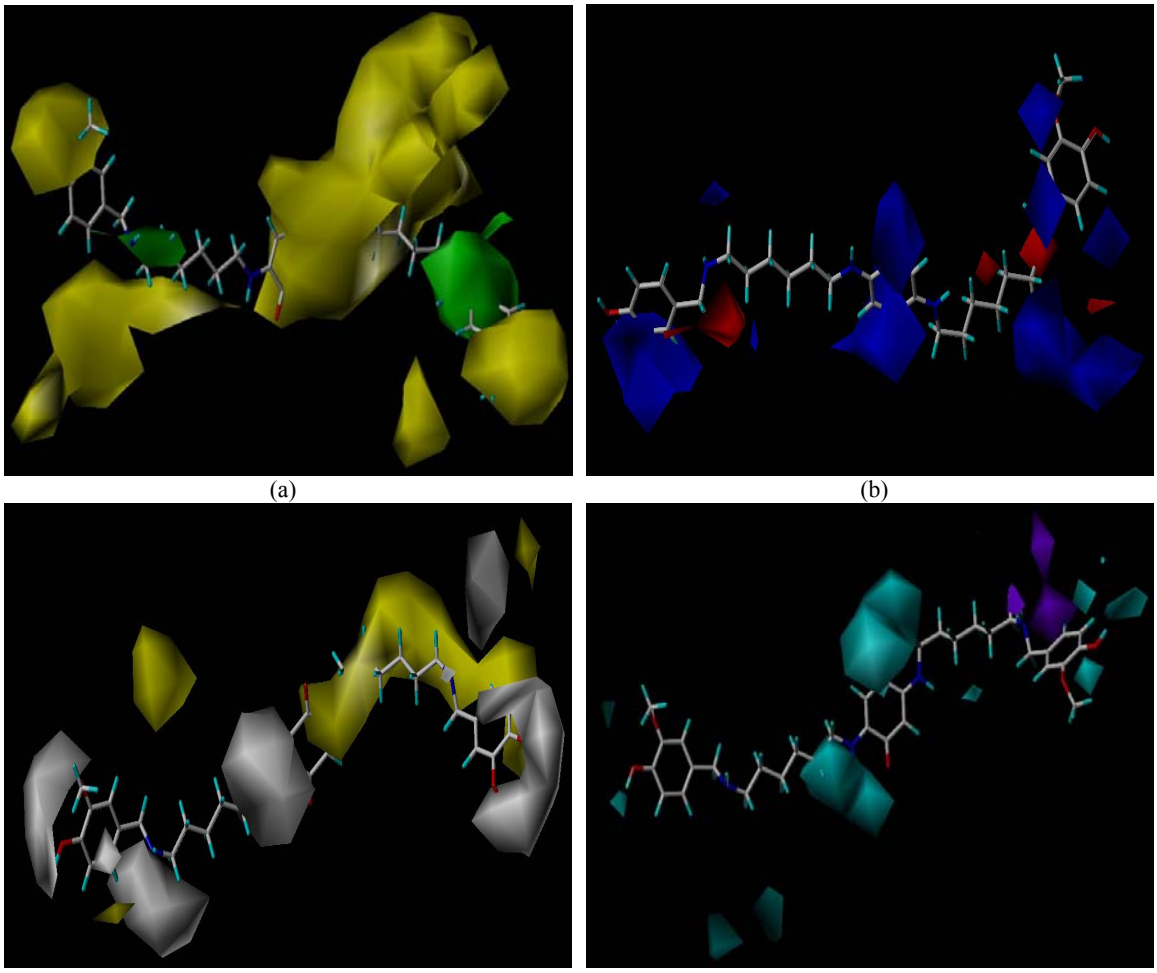

Fig. 3 CoMSIA contour maps around compound B2. (a) stereo field (green: steric favored; yellow: steric disfavored); (b) electrostatic field (blue: electropositive favored; red: electronegative favored); (c) hydrophobic field (yellow: hydrophobic favored; white: hydrophilic favored); (d) hydrogen bond donor field (cyan: hydrogen bond donor favored; purple: hydrogen bond donor disfavored).

3.2 Molecular Docking

3. 2. 1. Binding Mode with AChE

According to the Refs. [28-30], the active sites of AChE contain: (i) Catalytic triplets (SER203-GLU334-HIS447) and catalytic anionic sites (TRP86 and TYR337) which is located at the bottom of gorge; (ii) Peripheral anionic binding sites composed of residues TRP286 and TYR341 which is located at the entrance (mouth) of gorge. Our attention next turned toward the molecular docking with AChE, and three compounds (B1, B2 and B8) in Table 1 were selected as examples to illustrate the detailed interactions with AChE.

As shown in Table 1, the sequence of inhibitory activity was B2 > B1 > B8, while the sequence of total score was B1 > B8 > B2. In order to further clarify the results, we investigate the binding modes with AChE as shown in Fig. 4. For B2 (deep blue stick model), the whole molecule get stuck at the entrance of gorge (the peripheral site); for B1 (light blue bats model), the vanillic region is located at the entrance of gorge, and the others regions enter the gorge to interact with the catalytic active sites; for B8 (light blue stick model), the phenyl benzothiazole region enters the gorge to interact with the catalytic active sites, and the others regions get stuck at the entrance of gorge. Meanwhile, it could be observed from Fig. 4 that the

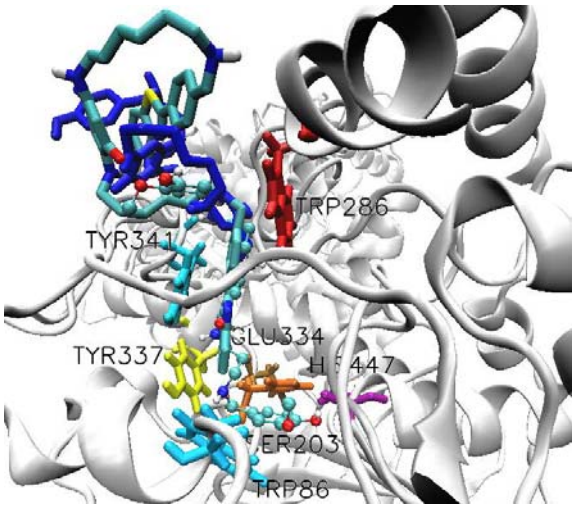

Fig. 4 Molecules and AChE docking schematic diagram. B2 (deep blue stick model); B1 (light blue bats model); B8 (light blue stick model).

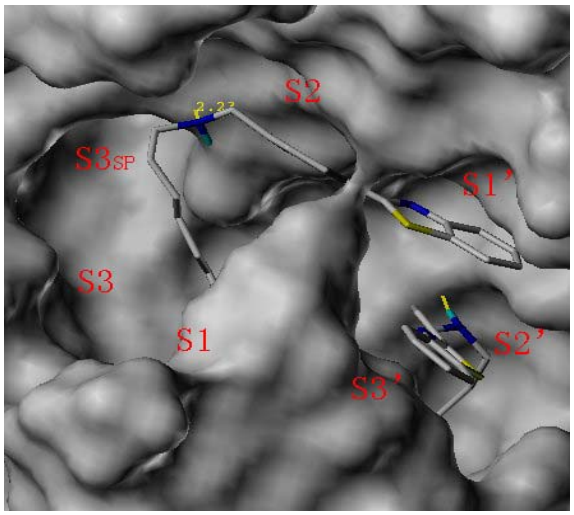

Fig. 5 The schematic diagram of B8 docking with BACE-1.

B1 enters the gorge to be more deeper than the B8. The result reveals that the total score might be dependent on the depth which inhibitor molecule enters the gorge, the deeper the molecule enters the gorge, the higher the total score would be. That explains why the sequence of total score was B1 > B8 > B2. However, the inhibitory activity had the order of B2 > B1 > B8, suggesting that the inhibitory activity should be determined by the interaction strength with AChE, the stronger the interaction would be, the higher the inhibitory activity would be. The result reflects that the peripheral site might be the important binding site for the inhibitory potency. Recent studies have also demonstrated that the peripheral site might accelerate the aggregation and deposition of beta-amyloid peptide, which is considered as another cause of AD [10, 31-33].

Based on above results, we can come to a conclusion that one side of inhibitor should be small volume group which could be easy to enter the gorge to interact with the catalytic active sites at the bottom of grge, and the other side of inhibitor should be large volume group which could interact strongly with the peripheral anionic sites at the entrance of gorge. The result is in well accordance with the CoMFA (Fig. 2a) and CoMSIA (Fig. 3a) steric contour plots obtained in 3D-QSAR studies.

3. 2. 2 Binding Mode with BACE-1

Up to now, crystal structure of the BACE-1 enzyme in complex with the different inhibitors have established its different binding subsites, i.e., S1 subsites include Leu30, Phe108, Typ115, and Ile118; S2 subsites include Arg235, Gln12, and Asn233; S3 subsites include Ala335, Ile110, and Ser113; S1' subsites include Lys224 and Thr329; and S2' subsites include Ile126 and Arg128 [34]. In this section, B8 in Table 1 was chosen as an example to characterize the binding mode with BACE-1. It could be observed from Fig. 5 that (i) the benzoquinone occupies the S1 pocket, (ii) six methylene occupy the S3' pocket, and the phenyl benzothiazole occupies the S2' pocket, (iii) the phenyl benzothiazole occupies the S1' pocket, (iv) the S3, S3sp, S2 pockets are empty. Huang et al. [35] stated that the S1, S2' and S3 active sites have the important role in improvement the inhibitory activity, and the S1, S2' and S3 pockets consist of largely hydrophobic environment. Therefore, if the hydrophobic substituents could occupy simultaneously S1, S2' and S3 pockets of BACE-1, a significant inhibitory potency would be increased.

Furthermore, as shown in Fig. 5, the active pockets of BACE-1 are all in the surface of protein, the S3 (including S3sp) pocket is wide, which is suitable for

bukly substituents, while the S2' pocket is narrow, which is suitable for small volume substituents. The result is in strong agreement with the CoMFA (Fig. 2a) and CoMSIA (Fig. 3a) steric contour plots obtained in 3D-QSAR studies.

4. Molecular Design

Based on the above results of 3D-QSAR model and molecular docking, we have designed eight novel multitargeted (AChE and BACE-1) inhibitors as shown in Table 3. One can observe from it that the predicted activities and total scores of eight designed molecules were all much larger than B2. In particular, F1 had the strongest predicted activity. F5 (binding with AChE) and E2 (binding with BACE-1) had the highest total scores, respectively.

In order to further clarify the results, the binding modes of F1, F5 and E2 with AChE were shown in Fig. 6. It could be observed from Fig. 6a that, F1 could enter the bottom of gorge to interact with the catalytic active sites (anionic site and triplets) so that the ACh (acetylcholine) hydrolysis might be prevented, and strong inhibitory activity of F1 might be achieved. As shown in Fig. 6b, it might be the

Table 3 The predicted activity by CoMFA model and respective docking score of putative AChE and BACE-1 binders.

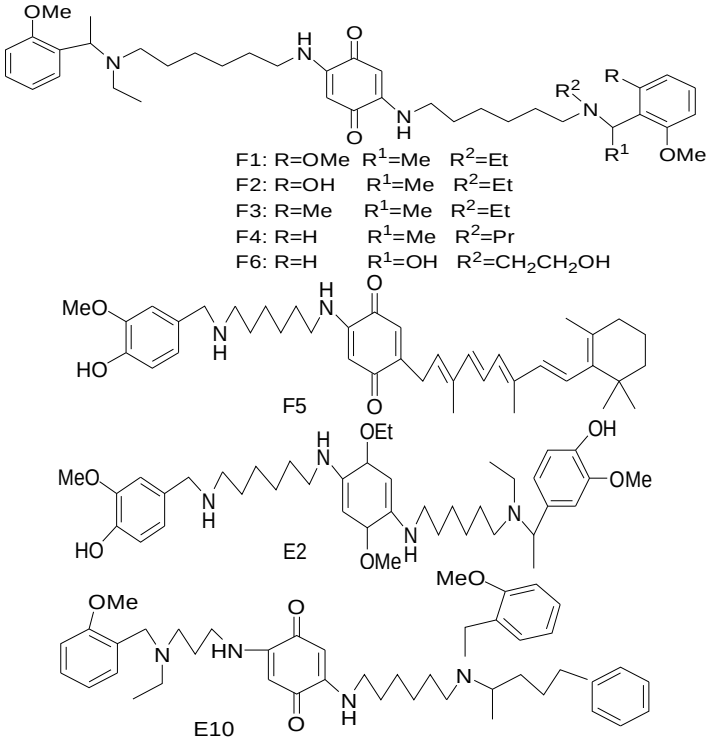

Name	Predicted activity (PIC_{50})	Total_Score (AChE)	Total_Score (BACE-1)
B2	6.979	4.53	6.76
F1	9.604	5.3718	10.7674
F2	9.592	7.6558	9.5085
F3	9.553	7.1444	7.7514
F4	9.527	11.3287	9.5614
F5	8.714	12.9844	10.9415
F6	8.201	11.5578	9.8724
E2	8.529	10.0777	14.2407
E10	8.190	8.6133	9.4063

(B2: The most potent inhibitor of B series in Table 1).

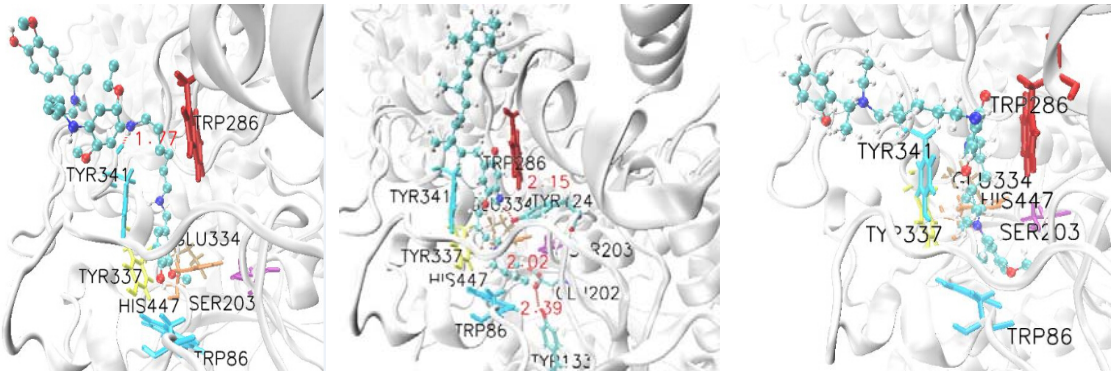

(a) (b) (c)

Fig. 6 The docking modes of designed molecules with AChE.

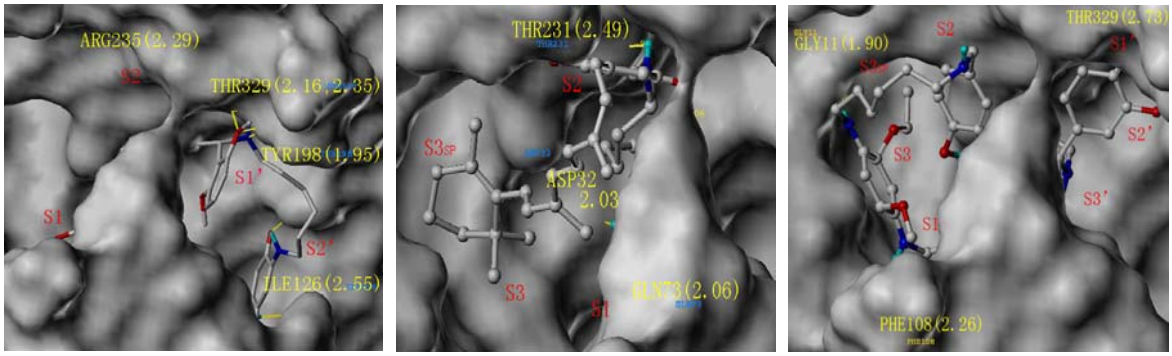

(a) (b) (c)

Fig. 7 The docking modes of designed molecules with BACE-1.

reason that F5 molecule is the planar conformation leading to the F5 would be advantageous to prevent ACh (acetylcholine) molecule into the gorge of AchE. The result is agreement with Chen and Ling's [36, 37] result, which the plane conformation of territrem B is the ensure of high inhibitory activity. Fig. 7 shows the binding modes of F1, F5 and E2 with BACE-1, respectively. It could be seen from it that F1 occupies S1 and S2' pockets, F5 occupies S3 pocket, E2 occupies simultaneously S2', S1 and S3 pockets so that its total score is the largest among eight designed molecules [35].

As mentioned above binding modes in Figs. 6 and 7, we found that the designed molecules in the present work could simultaneously bind to the catalytic and peripheral sites of AChE, which could disrupt the interactions between the AChE and ACh (acetylcholine), hence slow down the progression of the AD disease [10, 38, 39]. Furthermore, the designed molecules could also interact with dual targets (AChE and BACE-1) simultaneously. In particular, we hope that F1, F5 and E2 could be used as novel lead compounds on the biological experiment and further study.

The multifactorial nature of AD strongly supports the drug design strategy on MTDLs. Although this exciting new approach is still in its infancy [1, 40], and the selection of a therapeutic target is one of the biggest challenges in designing new molecules for this multifactorial disease [1, 41], it has opened a new avenue for the drug therapy of neurodegenerative diseases [1, 42]. In this respect, the road to developing new drugs based on the MTDLs strategy is still long, but it is highly conceivable that MTDLs may represent the future treatment for AD [1].

5. Conclusions

The 3D-QSAR model was established for 32 AD inhibitors by using CoMFA and CoMSIA techniques. Results showed that the CoMFA and CoMSIA models

were constructed successfully with a good cross-validated coefficient (q^2) and a non-cross-validated coefficient (R^2), the binding modes obtained by molecular docking were in agreement with the 3D-QSAR results, which demonstrates that the 3D-QSAR and docking models both have good predictive capability to guide the design and structural modification of multitargeted AD inhibitors. We found that, one side of inhibitory molecule should be small group so that it would be conductive to enter the gorge to interact with the catalytic active sites, and the other side of inhibitory molecule should be large group so that it would be favorable for interaction with the peripheral anionic sites. Furthermore, based on the 3D-QSAR model and the binding modes of AChE and BACE-1, the designed molecules could both act as dual binding sites (catalytic and peripheral sites of AChE) inhibitors and dual targets (AChE and BACE-1) inhibitors. We hope that our results could provide hints for the design of new multitargeted AD derivatives with high potency and specific activity.

Supplementary Information

(1) The 3-D structure of human AChE which includes a co-crystallized inhibitor donepezil (E20) has been determined by X-ray crystallography (J. Cheung, M. J. Rudolph, F. Burshteyn, M. S. Cassidy, E. N. Gary, J. Love, M. C. Franklin and J. J. Height, J. Med. Chem., 2012, 55, 10282-10286), and has been deposited in the Protein Data Bank with code 4EY7 (http://www.pdb.org/).

(2) The 3-D structure of human BACE-1 which includes a co-crystallized inhibitor AZD3835 (32D) has been determined by X-ray crystallography (Jeppsson, F., Eketjall, S., Janson, J., Karlstrom, S., Gustavsson, S., Olsson, L. L., Radesater, A. C., Ploeger, B., Cebers, G., Kolmodin, K., Swahn, B. M., Von Berg, S. Bueters, T., and Falting, J. J. Biol. Chem., 2012, 287, 41245-41257), and has been deposited in the Protein Data Bank with code 4B05 (http://www.pdb.org/).

Acknowledgments

The authors acknowledge the financial support of the Natural Science Foundation of Guangxi Province (No. 2013GXNSFAA019019) and the Natural Science Foundation of Guangxi Province (No. 2013GXNSFAA019041).

References

[1] Bolognesi, M. L., Rosini, M., Andrisano, V., Bartolini, M., Minarini, A., Tumiatti, V., and Melchiorre, C. 2009. "MTDL Design Strategy in the Context of Alzheimer's Disease: From Lipocrine to Memoquin and Beyond." *Current Pharmaceutical Design* 15: 601-13.

[2] Bolognesi, M. L., Bartolini, M., Tarozzi, A., Morroni, F., Lizzi, F., Milelli, A., Minarini, A., Rosini, M., Hrelia, P., Andrisano, V., and Melchiorre, C. 2011. "Multitargeted Drugs Discovery: Balancing Anti-amyloid and Anticholinesterase Capacity in a Single Chemical Entity." *Bioorganic and Medicinal Chemistry Letters* 21: 2655-8.

[3] Spilovska, K., Korabecny, J., Horova, A., Musilek, K., Nepovimova, E., Drtinova, L., Gazova, Z., Siposova, K., Dolezal, R., Jun, D., and Kuca, K. 2015. "Design, Synthesis and *in Vitro* Testing of 7-Methoxytacrineamantadine Analogues: A Novel Cholinesterase Inhibitors for the Treatment of Alzheimer's Disease." *Med. Chem. Res.* DOI 10.1007/s00044-015-1316-x (Published online: 29 January).

[4] Hui, A. L., Chen, Y., Zhu, S. J., Gan, C. S., Pan, J., and Zhou, A. 2014. "Design and Synthesis of Tacrine-Phenothiazine Hybrids as Multitarget Drugs for Alzheimer's Disease." *Med. Chem. Res.* 23: 3546-57.

[5] Rosini, M., Simoni, E., Minarini, A., and Melchiorre, C. 2014. "Multi-target Design Strategies in the Context of Alzheimer's Disease: Acetylcholinesterase Inhibition and NMDA Receptor Antagonism as the Driving Forces." *Neurochem. Res.* 39: 1914-23.

[6] Bolea, I., Gella, A., and Unzeta, M. 2013. "Propargylamine-derived multitarget-directed Ligands: Fighting Alzheimer's Disease with Monoamine oxidase Inhibitors." *J. Neural Transm.* 120: 893-902.

[7] Bolognesi, M. L., Bartolini, M., Rosini, M., Andrisano, V., and Melchiorre, C. 2009. "Structure-Activity Relationships of Memoquin: Influence of the Chain Chirality in the Multi-target Mechanism of Action." *Bioorganic and Medicinal Chemistry Letters* 19: 4312-5.

[8] Bolognesi, M. L., Chiriano, G. P., Bartolini, M., Mancini, F., Bottegoni, G., Maestri, V., Czvitkovich, S., Windisch,

M., Cavalli, A., Minarini, A., Rosini, M., Tumiatti, V., Andrisano, V., and Melchiorre, C. 2011. "Synthesis of Monomeric Derivatives to Probe Memoquin's Bivalent Interactions." *J. Med. Chem.* 54: 8299-304.

[9] Bolognesi, M. L., Cavalli, A., and Melchiorre, C. 2009. "Memoquin: A Multitarget-Directed Ligand as an Innovative Therapeutic Opportunity for Alzheimer's Disease." *Neurotherapeutics* 6: 152-62.

[10] Shen, L. L, Liu, G. X., and Tang, Y. 2007. "Molecular Docking and 3D-QSAR Studies of 2-Substituted 1-Indanone Derivatives as Acetylcholinesterase Inhibitors." *Acta Pharmacol. Sin.* 28: 2053-63.

[11] Kuntz, I. D. 1992. "Structure-Based Strategies for Drug Design and Discovery." *Science* 257: 1078-82.

[12] Drews, J. 2000. "Drug Discovery: A Historical Perspective." *Science* 287: 1960-4.

[13] Deb, P. K., Sharma, A., Piplani P., and Akkinepally, R. R. 2012. "Molecular Docking and Receptor-Specific 3D-QSAR Studies of Acetylcholinesterase Inhibitors." *Mol. Divers.* 16: 803-23.

[14] Steiner, S., and Anderson, N. L. 2000. "Pharmaceutical Proteomics." *AnnNY Acad Sci.* 919: 48-51.

[15] Graves, P. R., Kwiek, J. J., Fadden, P., Ray, R., Hardeman, K., Coley, A. M., Foley, M., and Haystead, T. A. 2002. "Discovery of Novel Targets of Quinoline Drugs in the Human Purine Binding Proteome." *Mol. Pharmacol.* 62: 1364-72.

[16] Bruneau, J. M., Maillet, J., and Tagat, E. 2003. "Drug Induced Proteome Changes in Candida Albicans: Comparison of the Effect of Beta (1, 3) Glucan Synthase Inhibitors and Two Triazoles, Fluconazole and Itraconazole." *Proteomics* 3: 325-36.

[17] Bolognesi, M. L., Cavalli, A., Bergamini, C., Fato, R., Lenaz, G., Rosini, M., Bartolini, M., Andrisano, V., and Melchiorre, C. 2009. "Toward a Rational Design of Multitarget-Directed Antioxidants: Merging Memoquin and Lipoic Acid Molecular Frameworks." *J. Med. Chem.* 52: 7883-6.

[18] SYBYL-X 2. 0, Tripos Inc., St. Louis, USA.

[19] Cheung, J., Rudolph, M. J., Burshteyn, F., Cassidy, M. S., Gary, E. N., Love, J., Franklin, M. C., and Height, J. J. 2012. "Structures of Human Acetylcholinesterasein Complex with Pharmacologically Important Ligands." *J. Med. Chem.* 55: 10282-6.

[20] Jeppsson, F., Eketjall, S., Janson, J., Karlstrom, S., Gustavsson, S., Olsson, L. L., Radesater, A. C., Ploeger, B., Cebers, G., Kolmodin, K., Swahn, B. M., Von Berg, S., Bueters, T., and Falting, J. 2012. "Discovery of Azd3839, a Potent and Selective Bace1 Clinical Candidate for the Treatment of Alzheimers Disease." *J. Biol. Chem.* 287: 41245-57.

[21] Pandey, A., Mungalpara, J., and Mohan, C. G. 2010. "Comparative Molecular Field Analysis and Comparative Molecular Similarity Indices Analysis of Hydroxyethylamine Derivatives as Selective Human BACE-1 Inhibitor." *Mol. Divers* 14: 39-49.

[22] Clark, M., Cramer, R. D., and Opdenbosch, V. N. 1989. "Validation of the General Purpose Tripos 5.2 Force Field." *J. Comput. Chem.* 10: 982-1012.

[23] Cramer, R. D., Bunce, J. D., and Patterson, D. E. 1988. "Cross-Validation, Bootstrapping, and Partial Least Squares Compared with Multiple Regression in Conventional QSAR Studies." *Quant. Struct-Act Relat.* 7: 18-25.

[24] Roy, P. P., and Roy, K. 2008. "On Some Aspects of Variable Selection for Partial Least Squares Regression Models." *QSAR Comb Sci.* 27: 302-13.

[25] Lv, Y. Y., Yin, C. S., Liu, H. Y., Yi, Z. S., and Wang, Y. 2008. "3D-QSAR Study on Atmospheric Half-Lives of POPs Using CoMFA and CoMSIA." *Journal of Environmental Sciences* 20: 1433-8.

[26] Roy, K. 2007. "On Some Aspects of Validation of Predictive Quantitative Structure-Activity Relationship Models." *Expert. Opin. Drug Discov.* 2: 1567-77.

[27] Xu, L., Wu, Y. P., Hu, C. Y., and Li, H. 2000. "Study on the Quantitative Structure-Activity about Structure-Toxicity of Aniline Compounds." *Science in China (Series B)* 30: 1-7.

[28] Nachon, F., Carletti, E., Ronco, C., Trovaslet, M., Nicolet, Y., Jean, L., and Renard, P. Y. 2013. "Crystal Structures of Human Cholinesterases in Complex with Huprine W and Tacrine: Elements of Specificity for Anti-Alzheimer's Drugs Targeting Acetyl-and Butyryl-Cholinesterase." *Biochem. J.* 453: 393-9.

[29] Carletti, E., Colletier, J. P., Dupeux, F., Trovaslet, M., Masson, P., and Nachon, F. 2010. "Structural Evidence that Human Acetylcholinesterase Inhibited by Tabun Ages through O-dealkylation." *J. Med. Chem.* 53: 4002-8.

[30] Bolognesi, M. L., Bartolini, M., Mancini, F., Chiriano, G., Ceccarini, L., Rosini, M., Milelli, A., Tumiatti, V., Andrisano, V., and Melchiorre, C. 2010. "Bis(7)-tacrine Derivatives as Multitarget-Directed Ligands: Focus on Anticholinesterase and Antiamyloid Activities." *Chem. Med. Chem.* 5: 1215-20.

[31] Silman I., and Sussman, J. L. 2005. "Acetylcholinesterase: "Classical" and "Nonclassical" Functions and Pharmacology." *Curr. Opin. Pharmacol.* 5: 293-302.

[32] Inestrosa, N. C., Alvarez, A., Pérez, C. A., Moreno, R. D., Vicente, M., Linker, C., Casanueva, O. I., Soto, C., and Garrido, J. 1996. "Acetylcholinesterase Accelerates Assembly of Amyloid-Beta-Peptides into Alzheimer's Fibrils: Possible Role of the Peripheral Site of the Enzyme." *Neuron* 16: 881-91.

[33] Bartolini, M., Bertucci, C., Cavrini, V., and Andrisano, V.

2003. "Beta-Amyloid Aggregation Induced by Human Acetylcholinesterase: Inhibition Studies." *Biochem. Pharmacol*. 65: 407-16.

[34] Ostermann, N., Eder, J., Eidhoff, U., Zink, F., Hassiepen, U., Worpenberg, S., Maibaum, J., Simic, O., Hommel, U., and Gerhartz, B. 2006. "Crystal Structure of Human BACE2 in Complex with a Hydroxyethylamine Transition-State Inhibitor." *J. Mol. Biol.* 355: 249-61.

[35] Huang, H. B., La, D. S., Cheng, A. C., Whittington, D. A., Patel, V. F., Chen, K., Dineen, T. A., Epstein, O., Graceffa, R., Hickman, D., Kiang, Y. H., Louie, S., Luo, Y., Wahl, R. C., Wen, P. H., Wood, S., Robert, T., and Fremeau, Jr. 2012. "Structure-and Property-Based Design of Aminooxazoline Xanthenes as Selective, Orally Efficacious, and CNS Penetrable BACE Inhibitors for the Treatment of Alzheimer's Disease." *J. Med. Chem.* 55: 9156-69.

[36] Chen, J. W., Luo, Y. L., Wang, M. J., Peng, F. C., Ling, K. H., and Territrem, B. 1999. "A Tremorgenic Mycotoxin that Inhibits Acetylcholinesterase with a Noncovalent yet Irreversible Binding Mechanism." *J. Biol. Chem.* 274: 34916-23.

[37] Ling, K. H., Chiou, C. M., and Tsneg, Y. L. 1991. "Biotransformation of Territrems by S9 Fraction from Rat Liver." *Drug Metab. Dispos.* 19: 587-95.

[38] Munoz-Muriedas, J., Lopez, J. M., Orozco M., and Luque, F. J. 2004. "Molecular Modelling Approaches to the Design of Acetylcholinesterase Inhibitors: New Challenges for the Treatment of Alzheimer's Disease." *Curr. Pharm. Des.* 10: 3131-40.

[39] Du, D. M., and Carlier, P. R. 2004. "Development of Bivalent Acetylcholinesterase Inhibitors as Potential Therapeutic Drugs for Alzheimer's Disease." *Curr. Pharm. Des.* 10: 3141-56.

[40] Weinreb, O., Amit, T., Bar-Am, O., Yogev-Falach, M., and Youdim, M. B. 2008. "The Neuroprotective Mechanism of Action of the Multimodal Drug Ladostigil." *Front Biosci.*13: 5131-7.

[41] Iqbal K., and Grundke-Iqbal, I. 2007. "Developing Pharmacological Therapies for Alzheimer Disease." *Cell. Mol. Life Sci.* 64: 2234-44.

[42] Espinoza-Fonseca, L. M. 2006. "The Benefits of the Multi-target Approach in Drug Design and Discovery." *Bioorg. Med. Chem.* 14: 896-97.